KA-TP-6-1996

Top pair production in e^+e^- collisions with virtual and real electroweak radiative corrections.*

V. Driesen, W. Hollik, A. Kraft

Institut für Theoretische Physik
Universität Karlsruhe, D-76128 Karlsruhe, Germany

February 1, 2008

Abstract

The effect of virtual electroweak corrections to $e^+e^- \to t\bar{t}$ and the contribution of the radiation processes $e^+e^- \to t\bar{t}Z, t\bar{t}H$ to the inclusive top pair production cross section and forward-backward asymmetry are discussed in the high energy regime.

*To appear in the Proceedings of the Workshop "Physics with e^+e^- Colliders", Annecy-Gran Sasso-Hamburg 1995, ed. P. Zerwas

Top pair production in e^+e^- collisions with virtual and real electroweak radiative corrections.

V. Driesen, W. Hollik, A. Kraft

Institut für theoretische Physik
Universität Karlsruhe
D-76128 Karlsruhe, Germany

Abstract

The effect of virtual electroweak corrections to $e^+e^- \to t\bar{t}$ and the contribution of the radiation processes $e^+e^- \to t\bar{t}Z, t\bar{t}H$ to the inclusive top pair production cross section and forward-backward asymmetry are discussed in the high energy regime.

For an accurate prediction of top pair production cross sections at a high energy e^+e^- collider, various types of higher-order effects have to be taken into account:

- the QCD corrections, which are treated perturbatively far from the threshold region, but require refinements on threshold and finite width effects close to the production threshold [1],
- the electromagnetic bremsstrahlung corrections (QED corrections) with real and virtual photons inserted in the Born diagrams. They are complete at the 1-loop level in the virtual and soft photon part [2] as well as in the hard photon contribution [3],
- the genuine electroweak corrections, which consist of all electroweak 1-loop contributions to $e^+e^- \to t\bar{t}$, without virtual photons in the external charged fermion self energies and vertex corrections. These are also available as a complete set of 1-loop contribution [2, 4, 5].

An important feature of the electroweak corrections is that they are large and negative at high energies far above the $t\bar{t}$ threshold, and thus lead to a sizeable reduction of the production cross-section. At very high energies, on the other hand, there are also radiation processes besides the conventional photon radiation which contribute to inclusive top pair production $e^+e^- \to t\bar{t}X$: The radiation of Z bosons (Fig. 1) and the radiation of Higgs bosons (Fig. 2).

In previous work [7, 8] these radiation processes were studied with emphasis on searches for Higgs bosons and on investigating the Yukawa interaction. They may, however, also be considered as contributions to the (inclusive) $t\bar{t}$ cross section at 1-loop order. Since they constitute a positive contribution, they increase the production rate of $t\bar{t}$ pairs according to $e^+e^- \to t\bar{t}(X)$ and hence compensate at least partially the negative terms from the virtual corrections.

In this note we present the influence of the virtual electroweak 1-loop corrections on top pair production and the contribution of $e^+e^- \to t\bar{t}Z, t\bar{t}H$ to the inclusive cross section and forward-backward asymmetry. In a first subsection the structure and size of the virtual

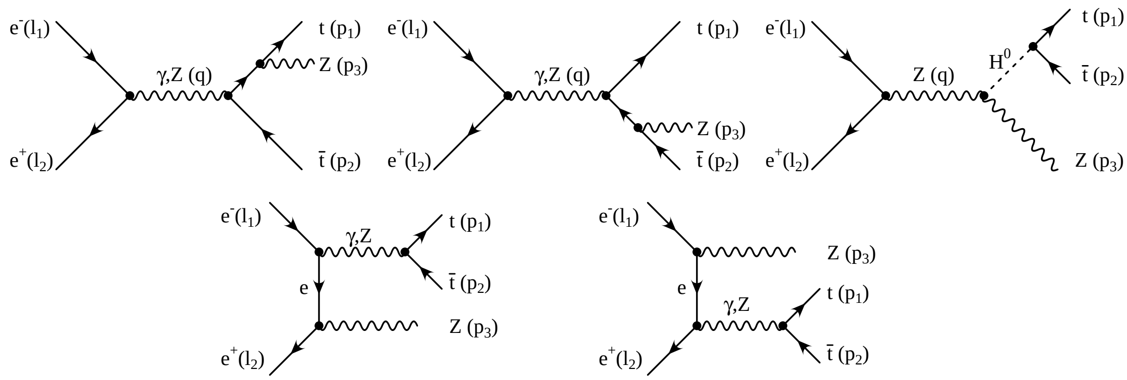

Figure 1: *Diagrams for* $e^+e^- \to t\bar{t}Z$*.*

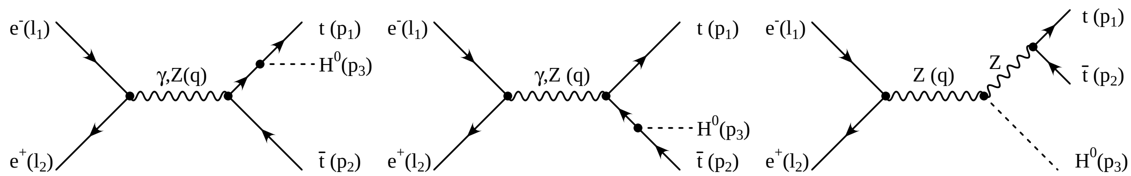

Figure 2: *Diagrams for* $e^+e^- \to t\bar{t}H$*.*

contributions are discussed. Subsequently, we include the Z and H radiation processes and show that the large and negative virtual contributions are sizeably compensated by including the Z,H bremsstrahlung processes.

Virtual contributions

The integrated cross section and the forward-backward asymmetry for the process $e^+(l_2)+e^-(l_1) \to t(p_1) + \bar{t}(p_2)$ with purely electroweak virtual corrections can be written in the form[1]

$$\begin{aligned} \sigma &= \frac{4\pi\alpha(s)^2}{3s}\, N_C\, \beta \left\{ \frac{1}{2}(3-\beta^2)\,\sigma_1(s) \,+\, \beta^2\,\sigma_2(s) \,+\, \Delta\sigma \right\} \\ A_{FB} &= \frac{3}{4}\beta \frac{\sigma_3 + \Delta\sigma'}{\frac{1}{2}(3-\beta^2)\,\sigma_1(s) \,+\, \beta^2\,\sigma_2(s) \,+\, \Delta\sigma} \end{aligned} \qquad (1)$$

where

$$\begin{aligned} & s = (p_1+p_2)^2, \\ & \beta = \sqrt{1-\frac{4m_t^2}{s}} \quad , \quad \alpha(s) = \frac{\alpha}{1+\hat{\Pi}^{\gamma}_{ferm}(s)} \equiv \frac{\alpha}{1-\Delta\alpha(s)}. \end{aligned} \qquad (2)$$

With $\hat{\Pi}^{\gamma}_{ferm} = \hat{\Pi}^{\gamma} - \hat{\Pi}^{\gamma}_{bos}$ we denote the fermionic part of the renormalized subtracted photon vacuum polarization. σ_1, σ_2, and σ_3 contain the lowest-order contribution and

[1] Up to $O(\alpha^4)$.

those one-loop corrections which can be incorporated in effective photon-fermion and Z-fermion couplings, i.e. the self-energies and the vertex corrections to the V, A couplings. The remaining terms, the top vertex corrections not of V, A structure and the contribution from the WW and ZZ box diagrams, are collected in $\Delta\sigma$ and $\Delta\sigma'$ for the symmetric and the antisymmetric cross section.

The σ_i can be written in the following way:

$$
\begin{aligned}
\sigma_1 &= \left(Q_e^{V\,2} + Q_e^{A\,2}\right)\, Q_t^{V\,2} \\
&\quad + 2\,(Q_e^V V_e + Q_e^A A_e)\, Q_t^V V_t\, \frac{s}{s-M_Z^2} \\
&\quad + \left(V_e^2 + A_e^2\right)\, V_t^2 \left(\frac{s}{s-M_Z^2}\right)^2 , \\
\sigma_2 &= Q_e^{V\,2}\, Q_t^{A\,2} \\
&\quad + 2\, Q_e^V V_e\, Q_t^A A_t\, \frac{s}{s-M_Z^2} \\
&\quad + \left(V_e^2 + A_e^2\right)\, A_t^2 \left(\frac{s}{s-M_Z^2}\right)^2 , \\
\sigma_3 &= 2 Q_e^V Q_t^V A_e A_t \frac{s}{s-M_Z^2} + 4 V_e V_t A_e A_t \left(\frac{s}{s-M_Z^2}\right)^2 .
\end{aligned} \tag{3}
$$

The effective coupling constants in these formulae are ($f = e, t$)

$$
\begin{aligned}
Q_f^V &= Q_f \left[1 - \frac{1}{2}\hat{\Pi}^{\gamma}_{bos}(s)\right] - F_V^{\gamma f}(s), \\
Q_f^A &= -F_A^{\gamma f}(s), \\
V_f &= \bar{v}_f + F_V^{Zf}(s), \\
A_f &= \bar{a}_f + F_A^{Zf}(s)
\end{aligned} \tag{4}
$$

with

$$
\begin{aligned}
\bar{a}_f &= \left(\frac{\sqrt{2} G_\mu M_Z}{4\pi\alpha(s)}\right)^{1/2} \bar{\rho}^{1/2}\, I_3^f \\
\bar{v}_f &= \left(\frac{\sqrt{2} G_\mu M_Z}{4\pi\alpha(s)}\right)^{1/2} \bar{\rho}^{1/2}\, (I_3^f - 2 Q_f \bar{s}^2)\, .
\end{aligned} \tag{5}
$$

They contain the propagator corrections

$$
\begin{aligned}
\bar{\rho} &= 1 - \Delta r - \hat{\Pi}^Z(s), \\
\bar{s}^2 &= s_W^2 - s_W c_W\, \hat{\Pi}^{\gamma Z}(s)
\end{aligned} \tag{6}
$$

with the self-energies renormalized according to the on-shell scheme

$$
\begin{aligned}
\hat{\Pi}^Z &= \mathrm{Re}\, \frac{\hat{\Sigma}^Z(s)}{s - M_Z}, \\
\hat{\Pi}^{\gamma Z} &= \mathrm{Re}\, \frac{\hat{\Sigma}^{\gamma Z}(s)}{s}\, ,
\end{aligned} \tag{7}
$$

together with the V, A form factors $F_{V,A}$ from the vertex corrections (real part). Δr is the radiative correction to the Fermi coupling constant in the on-shell scheme. The explicit expressions can be found in [2, 6].

The Born cross section $\sigma^{(0)}$ can be obtained from the formulae above by setting all the self-energies, vertex corrections, $\Delta\sigma$, $\Delta\sigma'$ and Δr in Eqs. (4-6) equal to zero.

The effect of the virtual electroweak corrections on the cross section for $e^+e^- \to t\bar{t}$ is displayed in Fig. 3, where the relative deviation from the "Born" cross section is shown. Note that "Born" already includes the QED running of the effective charge in the γ-exchange amplitude. The results in Fig. 3 are thus the residual corrections which are specific for the electroweak standard model.

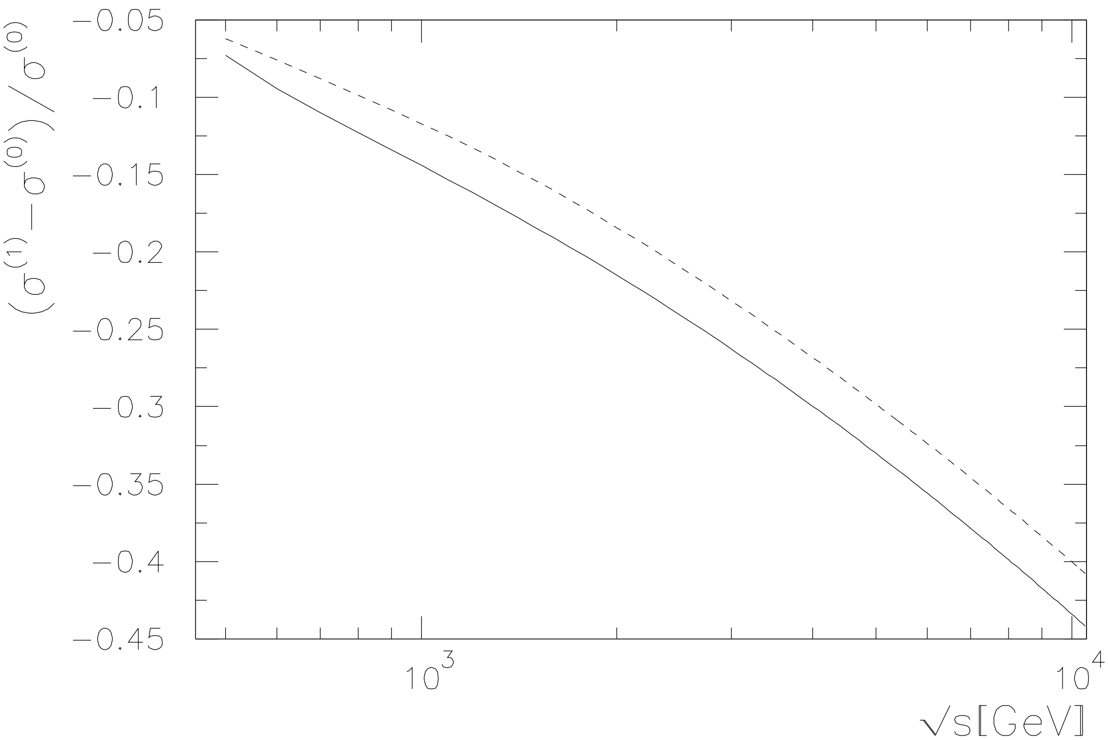

Figure 3: *Relative electroweak corrections to* $e^+e^- \to t\bar{t}$ *for* $M_H = 100\,\mathrm{GeV}$ *(solid line) and* $M_H = 1000\,\mathrm{GeV}$ *(dashed line).*

Real contributions

Next we consider the inclusive cross section for $t\bar{t}$ production in association with Higgs and Z bremsstrahlung. We thereby restrict our discussion to Higgs masses below $2m_t$, such that real Higgs production with subsequent decay into $t\bar{t}$ cannot occur. The latter case would be of specific interest for investigating the Higgs Yukawa interaction, and was explicitly studied in ref. [7].

The bremsstrahlung processes are of higher order in the coupling constants than the $2 \to 2$ process. The cross section at energies sufficiently above the threshold reach 10%

and more of the lowest order cross section. Their contribution to the $t\bar{t}$ final state hence becomes of the same order as the virtual electroweak corrections.

For the computation of the cross sections corresponding to the amplitudes in Figs. 1 and 2 the following set of couplings has been chosen:

$$\begin{aligned} \gamma f f &: \; -\sqrt{4\pi\,\alpha(s)}\;\gamma^\mu Q_f \\ Z f f &: \; -\sqrt{\sqrt{2}\,G_\mu\,M_Z^2}\;\gamma^\mu\;[(I_3 - 2Q_f\,s_w^2) - I_3\,\gamma_5] \\ H f f &: \; -\sqrt{\sqrt{2}\,G_\mu}\,m_f \\ H Z Z &: \; \sqrt{4\sqrt{2}\,G_\mu\,M_Z^2}\,M_Z \end{aligned}$$

For s_w^2 the approximate expression

$$s_w^2 = \frac{1}{2} - \sqrt{\frac{1}{4} - \frac{\pi\,\alpha(M_Z)}{\sqrt{2}\,G_\mu\,M_Z^2}} = 0.2311 \qquad (8)$$

is used.

In Fig. 4 we put together the integrated cross section for $e^+e^- \to t\bar{t}Z$ and $e^+e^- \to t\bar{t}H$ as function of the energy $\sqrt{s}$. The dominating contribution to the inclusive final state for $\sqrt{s} \geq 1$ TeV is from the "Z-strahlung", as can be seen from Fig. 4.

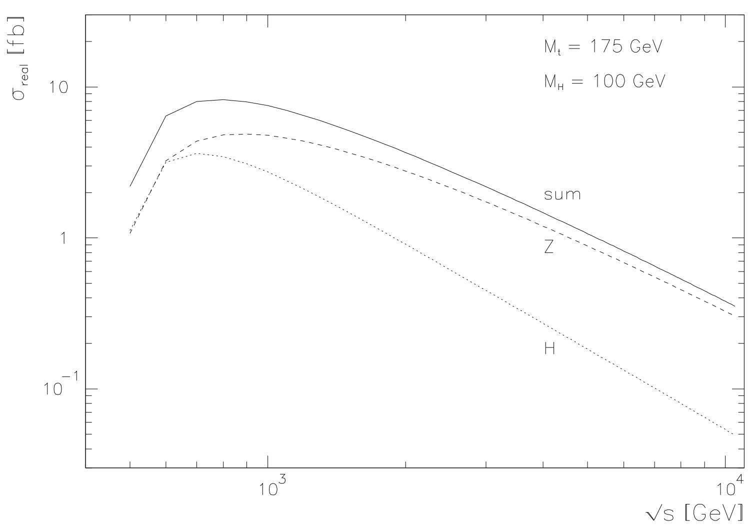

Figure 4: *Integrated cross section for* $e^+e^- \to t\bar{t}Z$ *and* $e^+e^- \to t\bar{t}H$*.*

We now can define an inclusive cross section for $t\bar{t}$ production in the following way:

$$\frac{d\sigma}{d\Omega}(t\bar{t}) = \frac{d\sigma_V}{d\Omega}(t\bar{t}) + \int d^3p_3 \frac{d\sigma(t\bar{t}H)}{d\Omega d^3p_3} + \int d^3p_3 \frac{d\sigma(t\bar{t}Z)}{d\Omega d^3p_3} \qquad (9)$$

where $d\Omega = d\cos\theta_t\ d\phi$ is the solid angle of the outgoing top, and θ_t the scattering angle between e^- and t. $d\sigma_V$ denotes the 2-particle final states including the virtual contributions, and d^3p_3 is the phase space element for H and Z, respectively.

The integrated cross section is obtained as

$$\sigma_{t\bar{t}} = \sigma_V(t\bar{t}) + \sigma(e^+e^- \to t\bar{t}H) + \sigma(e^+e^- \to t\bar{t}Z). \tag{10}$$

The forward-backward asymmetry A_{FB} is given by

$$A_{FB} \ = \ \frac{1}{\sigma_{t\bar{t}}}\left(\int_0^1 d\cos\theta_t \, \frac{d\sigma(t\bar{t})}{d\cos\theta_t} - \int_{-1}^0 d\cos\theta_t \, \frac{d\sigma(t\bar{t})}{d\cos\theta_t}\right) \tag{11}$$

with

$$\frac{d\sigma(t\bar{t})}{d\cos\theta_t} \ = \ \int_0^{2\pi} d\phi \, \frac{d\sigma}{d\Omega}(t\bar{t}) \tag{12}$$

The results are displayed in Figs. 5, 6. As one can see from Fig. 5, the virtual and real contributions to the integrated cross section cancel each other to a large extent. For A_{FB}, however, the situation is different. Fig. 6 contains A_{FB} in Born order, with virtual corrections, and after including the real contributions. For A_{FB}, the totally inclusive $t\bar{t}$ asymmetry deviates more from the Born result than the one with only virtual corrections to $e^+e^- \to t\bar{t}$.

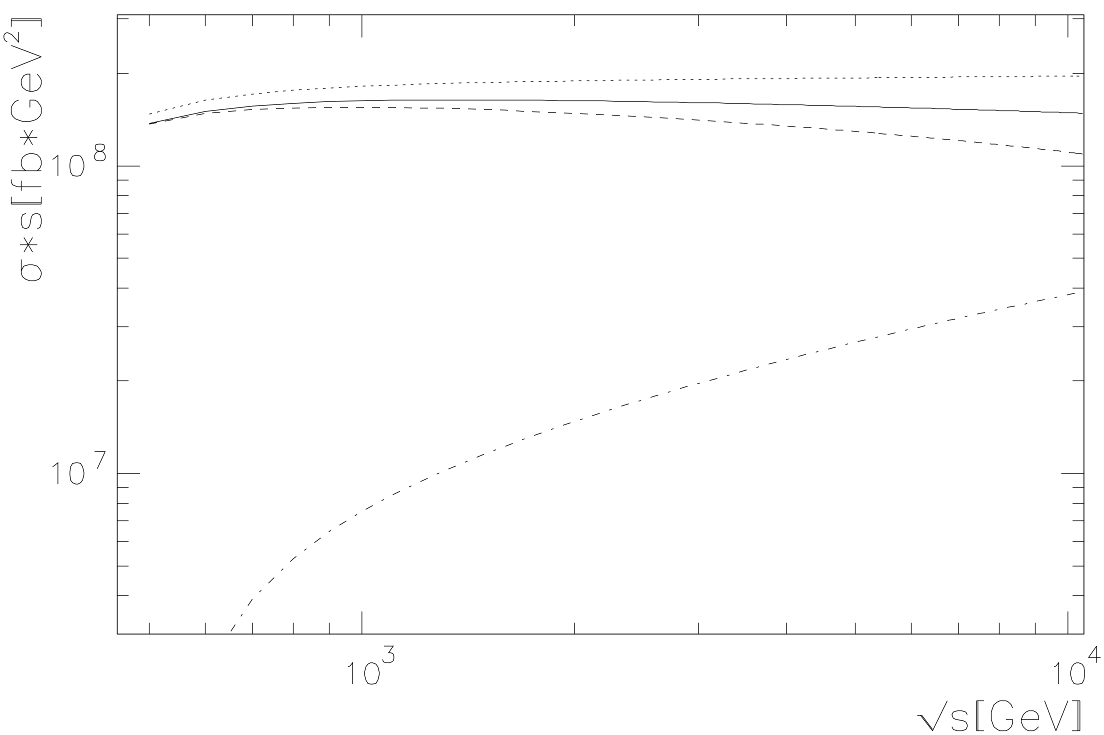

Figure 5: *Integrated cross section (times s). The dotted line shows the Born cross section $\sigma^{(0)}$, the dashed line contains all electroweak 1-loop virtual corrections, the dash-dotted line depicts the real contributions from $e^+e^- \to t\bar{t}H$ and $e^+e^- \to t\bar{t}Z$, and the solid line shows the inclusive cross section σ.*

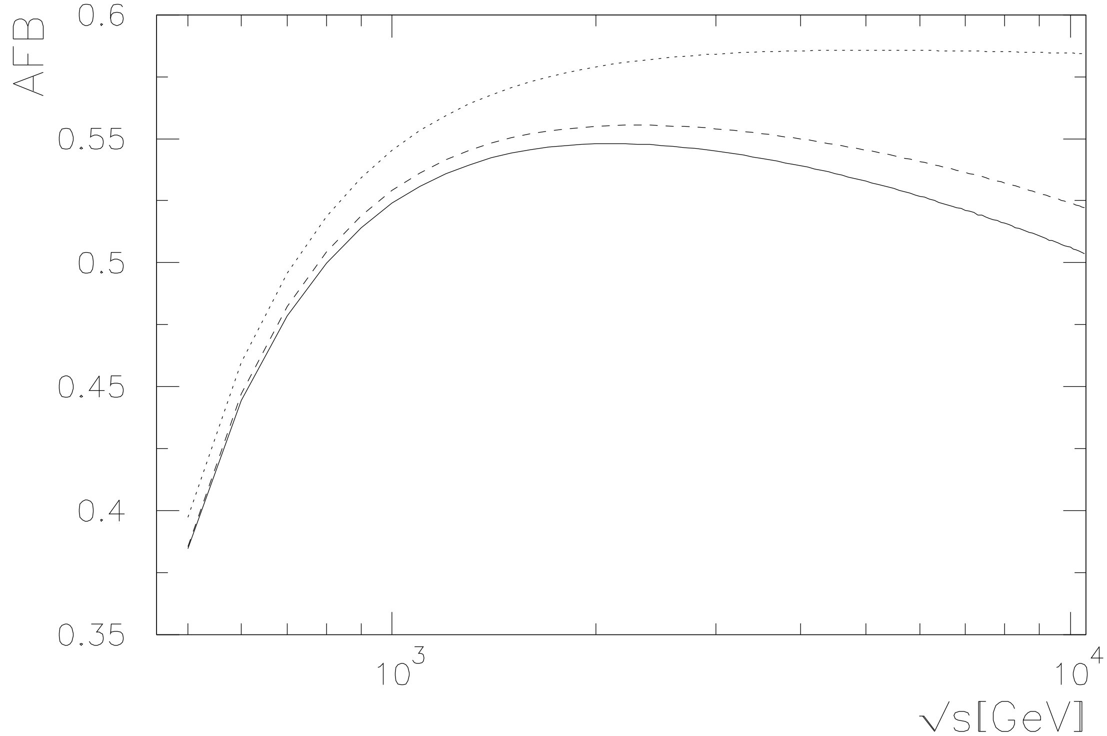

Figure 6: *Forward-backward asymmetry. The dotted line show the Born prediction, the dashed line contains also all electroweak 1-loop virtual corrections, and the solid line depicts the result for the inclusive production.*

Thereby, A_{FB} in Born approximation is obtained from Eq. (1) with expressions (3-6), where all self energies, vertex corrections, Δr and $\Delta\sigma$,$\Delta\sigma'$ are put to zero.

References

[1] J. Jersak, E. Laerman, P.M. Zerwas, *Phys. Rev.* **D25** (1980) 1218;
S. Güsken, J.H. Kühn, P.M. Zerwas, *Phys. Lett.* **B155** (1985) 185;
J.H. Kühn, P.M. Zerwas, *Phys. Rep.* **167** (1988) 321;
V.S. Fadin, V.A. Khoze, *Pi'sma v Zh. Eksp. Teor. Fiz.* **46** (1987) 417; *Yad. Fiz.* **48** (1988) 487;
V.S. Fadin, V.A. Khoze, T. Sjöstrand, *Z. Phys.* **C48** (1990) 613;
V.S. Fadin, O.I. Yakovlev, Novosibirsk preprint IYF 90-138 (1990);
W. Kwong, *Phys. Rev.* **D43** (1991) 1488;
H. Inazawa,, T. Morii, J. Morishita, *Phys. Lett.* **B203** (1988) 279; *Z. Phys.* **C42** (1989) 569;
K. Hagiwara et al., *Nucl. Phys.* **B344** (1990) 1;
J. Feigenbaum, *Phys. Rev.* **D43** (1991) 264;
M.J. Strassler, M.E. Peskin, *Phys. Rev.* **D43** (1991) 1500;
J.H. Kühn, Proceedings of the *Workshop on on Physics and Experiments with Linear e^+e^- Colliders*, Waikoloa, Hawaii 1993, eds.: F.A. Harris, S.L. Olsen, S. Pakvasa, X. Tata

[2] W. Beenakker, W. Hollik and S.C. van der Marck, *Nucl. Phys.* **B365** (1991) 24.

[3] A.A. Akhundov, D.Y. Bardin and A. Leike, *Phys. Lett.* **B261** (1991) 321;
A. Arbuzov, D. Bardin, A. Leike, *Mod. Phys. Lett.* **A7** (1992) 2029; E: **A9** (1994) 1515.

[4] W. Beenakker and W. Hollik, *Phys. Lett.* **B269** (1991) 425.

[5] W. Beenakker, A. Denner and A. Kraft, *Nucl. Phys.* **B410** (1993) 219.

[6] W. Hollik, *Fortschr. Phys.* **38** (1990) 165;
M. Consoli, W. Hollik, F. Jegerlehner, in: Z Physics at LEP1, CERN 89-08(1989), eds. G. Altarelli, R. Kleiss, C. Verzegnassi.

[7] K. Hagiwara, H. Murayama, I. Watanabe, *Nucl. Phys.* **B367** (1991) 257.

[8] A. Djouadi, J. Kalinowski, P.M. Zerwas, *Z. Phys.* **C54** (1992) 255